Systematic theoretical investigation for adsorption behavior of Al and N atoms on 4H-SiC$(11\bar{2}0)$ surfaces

Takumi Ito, Toru Akiyama, Kohji Nakamura and Tomonori Ito

Department of Physics Engineering, Mie University,

1557 Kurima-Machiya, Tsu, Mie 514-8507, Japan

Abstract

We systematically investigate adsorption behavior of Al and N atoms on 4H-SiC $(11\bar{2}0)$ surfaces based on first-principles calculations. The calculations for stable adsorption site demonstrate that the Al atom is adsorbed at the lattice site of 4H structure whereas the N atom is incorporated at the interstitial site. The calculated surface phase diagrams for Al and N atoms as functions of beam equivalent pressure and temperature clarify that Al atoms can be adsorbed at all of adsorption sites below 1800 K and N atoms, in contrast, are desorbed excepting the most stable site above 1150 K. These temperatures imply that under experimental conditions (1223 K) Al atoms can be easily adsorbed and N atoms are adsorbed only on the most stable adsorption site. Furthermore, the calculated barrier height of adsorbed Al and N atoms are 1.0 and 1.8 eV, respectively, implying that the surface migration of Al atoms is prominent compared to that of N atoms. These results obtained thus manifest that adsorption behavior of Al and N atoms are quite different and the growth processes change depending on V/III ratio under molecular beam epitaxy growth.

PACS Codes: 68.43.Bc, 81.05.Ea, 81.10Aj

Keywords: nonpolar surface; AlN; SiC; *Ab initio* calculation; adsorption; desorption

Corresponding author: Takumi Ito

Contact address: Department of Physics Engineering, Mie University, 1557 Kurima-Machiya, Tsu, Mie 514-8507, Japan

TEL: +81-59-232-1211

FAX: +81-59-231-9726

E-mail: ito06@nd.phen.mie-u.ac.jp

1. Introduction

Group-III nitrides (III-N) such as AlN, GaN, and InN with nonpolar orientations are of importance for potential applications in high-efficiency light-emitting devices.[1–4] In particular, AlN films with nonpolar orientations have been paid much attention to the applications of ultra-violet optoelectronic devises. The growth of non-polar AlN is generally investigated for 2H(wurtzite)-AlN on various substrates such as 6H-SiC(11-20). [5] However, the 2H-AlN is very defective due to lattice mismatch, structural mismatch. It contains many stacking faults and threading dislocations.

As an alternative approach, the growth of 4H-AlN on 4H-SiC substrate has been recently performed [6] and very high-quality 4H-AlN can be realized by precise tuning of V/III ratios and SiC surface treatment using plasma assisted molecular beam epitaxy (MBE). [7,8] This implies that the influence of the V/III ratio on polytype of AlN($11\bar{2}0$) grown on 4H-SiC($11\bar{2}0$) substrate: For N-rich condition 2H-AlN films are grown on the substrate while 4H-AlN films are formed under Al-rich condition: The growth mechanisms of AlN films on the 4H-SiC substrate are influenced on the V/III ratio. However, the growth processes such as adsorption-desorption behavior of Al and N atoms and their surface migrations on 4H-SiC($11\bar{2}0$) have been rarely investigated at present.

In our previous studies, we have successfully investigated adsorption behavior on the GaAs (001)–c(4×4) and GaAs(111)*B* surfaces using our *ab initio*-based approach in which surface phase diagram depending on temperature and pressure is described by comparing the calculated adsorption energy with chemical potential estimated by quantum statistical mechanics[9,10]. In this study, we extend our approach to clarify the adsorption-desorption behavior of Al and N atoms and their migration on the 4H-SiC($11\bar{2}0$) surfaces. Based on the calculated results, the growth processes of AlN films with different crystal structure depending on the V/III ratio are also inferred.

2. Computational methods

The calculations are based on the generalized gradient approximation.[11] We use norm-conserving pseudopotentials for Al, Si and H atoms [12] and ultrasoft pesudopotentials for N and C atoms.[13] The conjugate-gradient technique [14, 15] is utilized both for the electronic structure calculation and for the geometry optimization. The valence wave functions are expanded by the plane-wave basis set with a cutoff energy of 25 Ry, which gives an enough convergence of total energy to discuss the relative stability.

Figure 1 shows top and side views of 4H-SiC $(11\bar{2}0)$ surface model considered in this study. In order to avoid interactions between adjacent unit cells, we use a large unit cell in which the lengths along the $[1\bar{1}00]$ and [0001] directions are 10.77 and 10.07 Å. We take slab models consisting of four monolayers with hydrogen atoms and vacuum region equivalent to 6 monolayers thicknesses (~8 Å). The atoms belonging to the bottom bilayer are fixed at their ideal position. To determine adsorption-desorption behavior, we put an adsorbent (Al or N atom) for various sites. These sites are prepared by making two-dimensional meshes with intervals of 0.89 and ~0.94 Å along the $[1\bar{1}00]$ and [0001] directions, respectively. We perform the calculations where the adsorbent is put on each mesh-point and the geometry is optimized imposing a constraint for the adsorbent perpendicular to the surface. We thus obtain 36 different configurations for each adsorbed atom and determine the most stable adsorption site. Furthermore, we construct two-dimensional energy contour plots to obtain the migration behavior of adsorbed atom.

The adsorption–desorption behavior depending on temperature and beam equivalent pressure (BEP) can be described by comparing the free energy of ideal gas per one particle (chemical potential) μ_{gas} with the adsorption energy μ_{solid}. Here, the adsorption energy μ_{solid} is calculated according to the following equation:

$$\mu_{solid} = E_{total} - E_{sub} - E_{atom},$$

where E_{total} is the total energy of the surface with adsorbent, Esub the total energy of the surface without adsorbent, and E_{atom} is the total energy of isolated atom. The chemical potential μ_{gas} of the ideal gas is given by the following equation [16,17]:

$$\mu_{gas} = -k_B T \ln\left[k_b T / p \times (2\pi m k_b T / h^2)^{3/2}\right].$$

Here, k_B is Boltzmann's constant, T the gas temperature, g the degree of degeneracy of electron energy level, p the beam equivalent pressure of the particle, m the mass of one particle, and h the Planck's constant. That is, the structure corresponding to adsorbed surface is favorable when μ_{solid} is less than μ_{gas}, whereas desorbed surface is stabilized when μ_{gas}, is less than μ_{solid}.

3. Results and discussion

Figure 2 shows the calculated contour plots of the energy for Al and N adatoms on the 4H-SiC $(11\bar{2}0)$ substrate. As shown in Fig. 2(a), the energetically lowest position for the Al atom is located close to the lattice site of C atom. On the other hand, the N atom has the lowest energy when it is located at the interstitial site above the top C atom [Fig. 2(b)]. This implies that stable adsorption sites for Al and N atoms are different. These stable sites can be explained in terms of the electron counting model (ECM). [18] For 4H-SiC $(11\bar{2}0)$ surface without adsorbents, all dangling bonds of Si atoms are empty and those of C atoms are fully occupied by electrons. [19] Due to the transfer of electrons, the surface becomes semiconducting and stabilized. When the Al atom is adsorbed at the stable site, it forms two Al-C bonds and an Al-Si bond with its nearest neighbor C and Si atoms, respectively. Thus, the Al atom forms in total three covalent bonds whereas only less than two bonds are formed on the other adsorption site. Due to the formation of three covalent bonds, the number of excess electrons becomes only one in the unit cell. However, this adsorption site (where two C-N bonds and a Si-N bond are formed) is not the stable site for the N atom because the N atom can form two Si-N bonds and a C-N bond at the interstitial site. Since the bond energy

of Si-N is small compared to that of C-N, [20] larger number of Si-N bonds causes the stabilization of the N atom. Table I shows the calculated adsorption energy for the Al and N atoms. We note that the adsorption energy corresponds to the geometry which is calculated without any constraints for the adsorbents. The adsorption energy of the Al atoms is found to be lower than that of the N atoms. This implies that the adsorption of Al atoms is more favorable than that of N atoms.

From Fig. 2, furthermore, we can obtain the migration behavior of adsorbed Al and N atoms. For the Al atom, symmetrically equivalent stable sites are placed with ~5.3 Å interval. If we assume that the migration occurs by taking the migration pathways between nearest-neighbor stable sites, the migration barrier corresponds to the highest total energy position along the ridge between nearest neighbor-stable sites. Table I also shows the energy barriers based on this assumption. We obtain the values of 1.11 and 0.92 eV along the $[1\bar{1}00]$ and [0001] directions, respectively: It seems that the migration along the [0001] direction [arrow in Fig. 2(a)] is slightly easier than that along the $[1\bar{1}00]$ direction [dotted arrow in Fig. 2(a)]. The low migration energy barrier along the [0001] direction for the Al atom can be understood by the shorter distance between stable or metastable positions along the migration pathways. For instance, the distances along the [0001] direction for the Al (N) atom are ~1.88 (2.63) Å whereas those along the [1-100] direction are ~5.26 (3.01) Å. For the N atom, the migration barriers are higher than those for Al atoms. Again, the migration along the [0001] direction of N atoms [arrow in Fig. 2(b)] is easier than that along the $[1\bar{1}00]$ direction [dotted arrow in Fig. 2(b)]. Since the C-N and Si-N bonds are short (1.45 and 1.83 Å, respectively) compared to Al-C and Al-C bonds (2.07 and 2.45 Å), breaking of the C-N bond occurs at the transition state for the migration along the $[1\bar{1}00]$ direction. This migration corresponds to a jumping process through the trench located between top surfaces. In contrast, the migrations along the [0001] direction coincide with the atomic arrangement of the top surface. Along this direction, breaking and formation of Si-N and C-N bonds occur simultaneously, resulting in lower migration barrier.

To clarify the adsorption-desorption behavior under the MBE conditions, we calculate

surface phase diagrams of Al and N atoms on the surface. Figures 3(a) and 3(b) show the calculated phase diagram for the adsorption of Al and N atoms as functions of temperature and Al- and N-BEP, respectively. As shown in Fig. 3(a), the desorption temperature of the Al atom changes from 1800 to 2370 K depending on Al-BEP. These values are much higher than the experimental conditions (1223 K). Furthermore, even in the metastable sites, the desorption temperature for surface phase transition (1750-2300 K) is much higher than the experimentally reported temperature. From these findings, we can derive that the Al atom is adsorbed every adsorption site and migrate without desorption. On the other hand, the desorption temperature of the N atom which is located at the most stable site changes from 1100 to 1500 K. By comparing the calculated temperature range for adsorption with the experiment, the N atom is adsorbed at the stable site when N-BEP is larger than 1×10^{-6} Torr. However, the desorption temperature for the N atom located at metastable sites becomes lower than that at the most stable site. As a result, the N atom located at metastable sites is desorbed over wide range of N-BEP. Therefore, the N atom can be adsorbed only at the most stable site and is desorbed during its migration toward other adsorption sites. These results thus indicate that the adsorption-desorption behavior of Al and N atoms are quite different with each other.

Based on the calculated results, we can furthermore conjecture the growth processes of AlN films with different crystal structure depending on the V/III ratio. [7,8] If we assume that the growth under Al-rich condition is dominated by Al atoms, this growth can be interpreted in terms of the adsorption behavior of Al atoms. Since the Al atom is adsorbed close to the lattice site of 4H-SiC, it is likely that the growing AlN films inherit the atomic arrangement of the substrate, resulting in the formation of 4H-AlN. For N-rich condition, in contrast, we can consider that the growth is dominated by N atoms. Since the N atoms is unable to be adsorbed at the lattice site of the substrate but incorporated at the interstitial site, the growing AlN films are likely not to inherit the atomic arrangement of the substrate and then the most stable crystal structure (2H-AlN) can be formed. Although details of the AlN growth processes on SiC $(11\bar{2}0)$ substrate should be verified more quantitatively, this is reasonably consistent with

the experimental fact that 2H (4H)-AlN films are grown under N (Al)-rich condition. [7,8]

4. Conclusion

We have investigated adsorption behavior of Al and N atoms on the 4H-SiC ($11\bar{2}0$) surface based on first-principles calculations. We have found that the Al atom is adsorbed at the lattice site of 4H structure whereas the N atom is adsorbed at the interstitial site. The calculated surface phase diagrams for Al and N atoms as functions of beam equivalent pressure and temperature clarify that Al atoms can be adsorbed at all of adsorption sites below 1800 K and N atoms in contrast are desorbed excepting the most stable site above 1150 K. These temperatures imply that under experimental conditions (1200 K) Al atoms can be easily adsorbed and N atoms are incorporated only on the stable adsorption site. The calculated energy barrier for the surface migration of adsorbed Al and N atoms are 1.0 and 1.8 eV, respectively, implying that the migration of Al atoms is prominent compared to that of N atoms. These results obtained thus suggest that adsorption behavior of Al and N atoms are quite different and the growth processes changes depending on V/III ratio under MBE growth.

Acknowledgments

This work was supported in part by Grant-in-Aid for Scientific Research from JSPS under contracts No. 18560020. Computational were performed at RCCS (National Institute of Sciences) and ISSP (University of Tokyo).

References

[1] P. Waltereit, O. Brandt, A. Trampert, H. T. Grahn, J. Menniger, M. Ramsteiner, M. Reiche, K. H. Ploog, Nature **406** (2000) 865.

[2] H. M. Ng, Appl. Phys. Lett. **80** (2002) 4369.

[3] B. A. Haskell, F. Wu, M. D. Craven, S. Matsuda, P. T. Fini, T. Fujii, K. Fujito, S. P. Denbaars, J. S. Speck, S. Nakamura, Appl. Phys. Lett. **83** (2003) 644.

[4] O. Brandt, Y. J. Sun, L. Däweritz, K. H. Ploog, Physica E **23** (2004) 339.

[5] N. Onojima, J. Suda, and H. Matsunami, Jpn. J. Appl. Phys. 41, L1348 (2002).)

[6] N. Onojima, J. Suda, H. Matsunami, Appl. Phys. Lett. **83** (2003) 5208.

[7] M. Horita, J. Suda, T. Kimoto, Phys. Stat. Sol. (c) **3** (2006) 1503.

[8] J. Suda, M. Horita, R. Armitage, T. Kimoto, J. Crst. Growth **301**-**302** (2007) 410.

[9] T. Ito, K. Tsutsumida, K. Nakamura, Y. Kangawa, K. Shiraishi, A. Taguchi, H. Kageshima, Appl. Surf. Sci. **237** (2004) 194.

[10] H. Tatematsu, K. Sano, T. Akiyama, K. Nakamura, T. Ito, Phys. Rev. B **77** (2008) 233306.

[11] J. P. Perdew, K. Burke, M. Ernzerhof, Phys. Rev. Lett. **77** (1996) 3865.

[12] N. Troullier, J. L. Martins, Phys. Rev. B **43** (1991) 1993.

[13] D. Vanderbilt, Phys. Rev. B **43** (1990) 7892.

[14] J. Yamauchi, M. Tsukada, S. Watanabe, O. Sugino, Phys. Rev. B **54** (1996) 5586.

[15] H. Kageshima, K. Shiraishi, Phys. Rev. B **56** (1997) 14985.

[16] Y. Kangawa, T. Ito, A. Taguchi, K. Shiraishi, T. Ohachi, Surf. Sci **493** (2001) 178.

[17] Y. Kangawa, T. Ito, Y. S. Hiraoka, A. Taguchi, K. Shiraishi, T. Ohachi, Surf. Sci **507**-**510** (2002) 285.

[18] M. D. Pashley, Phys. Rev. B **40** (1989) 10481.

[19] The ideal surface satisfies the ECM by considering electron transfer from Si dangling bonds to C dangling bonds, so that the ideal surface can be considered as a stable surface structure on nonpolar orientation. Indeed, we find from the surface band structure that

the electronic states caused by C dangling bond are fully occupied and those by Si dangling bond are empty. This band structure characteristics can be interpreted as lower carbon sp^3 orbital compared to silicon sp^3 orbital.

[20] T. Araki, T. Akiyama, K. Nakamura, T. Ito, e-J. Surf. Sci. Nanotec. **3** (2005) 507.

Figure Captions

FIG 1: (a) Top and (b) side views of 4H-SiC $(11\bar{2}0)$ surface considered in this study. White and black circles represent C and Si atoms, respectively. Small grey circles are H atoms terminating bottom surface. Dotted line denotes the surface unit cell.

FIG. 2: Contour plots of total energies for (a) Al and (b) N adatoms on 4H-SiC $(11\bar{2}0)$ surfaces. The origin of energy is set to the total energy of the most stable site. The notation of Si and C atoms is the same as in Fig. 1. Open circles represent the adsorbed atoms.

FIG. 3: Calculated surface phase diagrams of adsorbed (a) Al and (b) N atoms as functions of temperature and BEP, along with their atomic structures. Dashed line represents the growth temperature of AlN films in the MBE. The phase boundary for the adsorbed N atom for the metastable structure is shown by dotted line.

FIG. 1

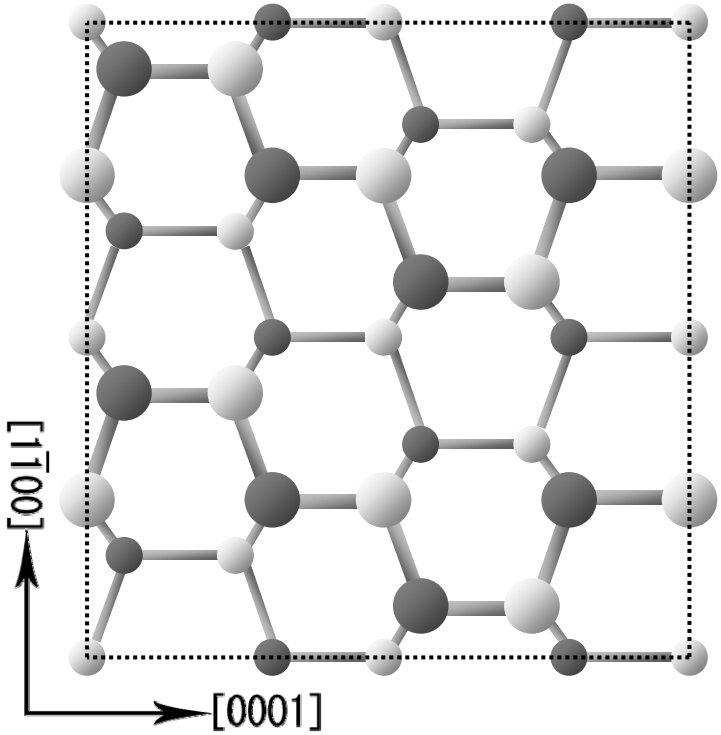

(a)

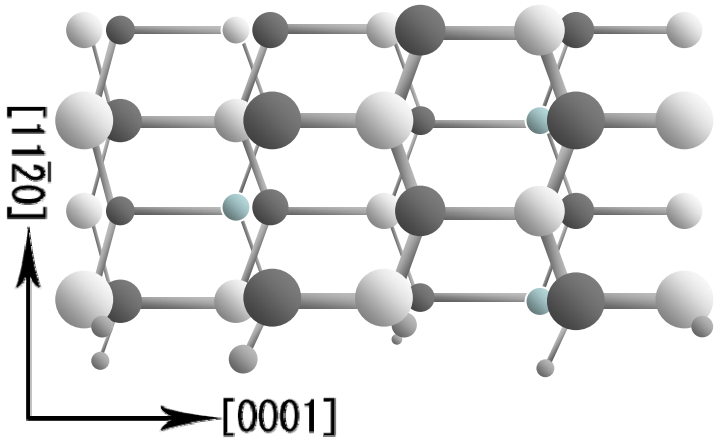

(b)

Si C H

FIG. 2

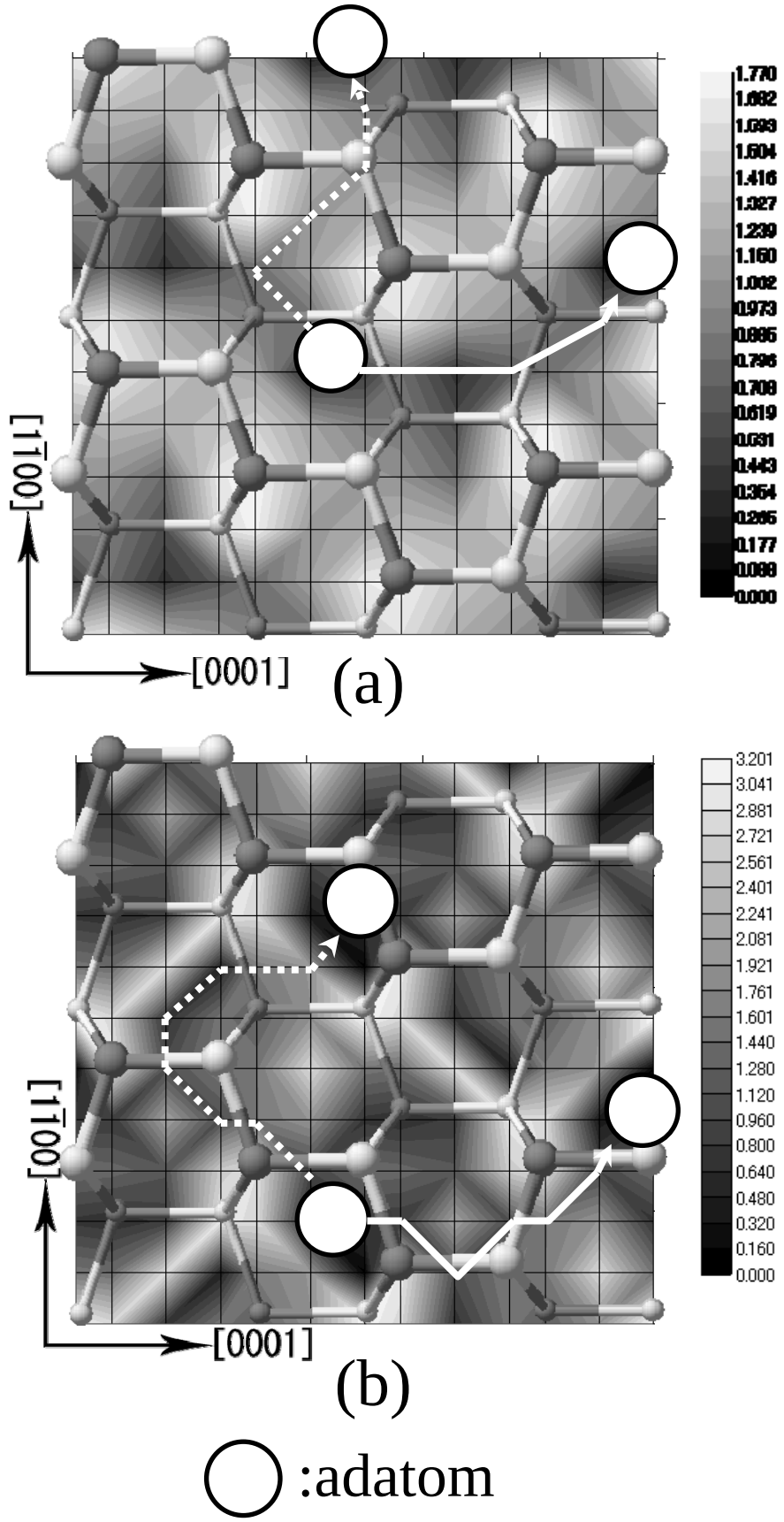
1.770
1.682
1.593
1.504
1.416
1.327
1.239
1.160
1.002
0.973
0.885
0.796
0.708
0.619
0.531
0.443
0.354
0.265
0.177
0.088
0.000
[1$\bar{1}$00]
[0001]
(a)
3.201
3.041
2.881
2.721
2.561
2.401
2.241
2.081
1.921
1.761
1.601
1.440
1.280
1.120
0.960
0.800
0.640
0.480
0.320
0.160
0.000
[1$\bar{1}$00]
[0001]
(b)
:adatom

Table I

Table I : Calculated adsorption energy E_{ad} and migration energy barrier E_b along the [0001] and $[1\bar{1}00]$ directions. The unit of energy is eV.

	Al	N
E_{ad}	-6.71	-4.06
E_b along [0001]	0.92	1.59
E_b along $[1\bar{1}00]$	1.11	1.95

FIG. 3

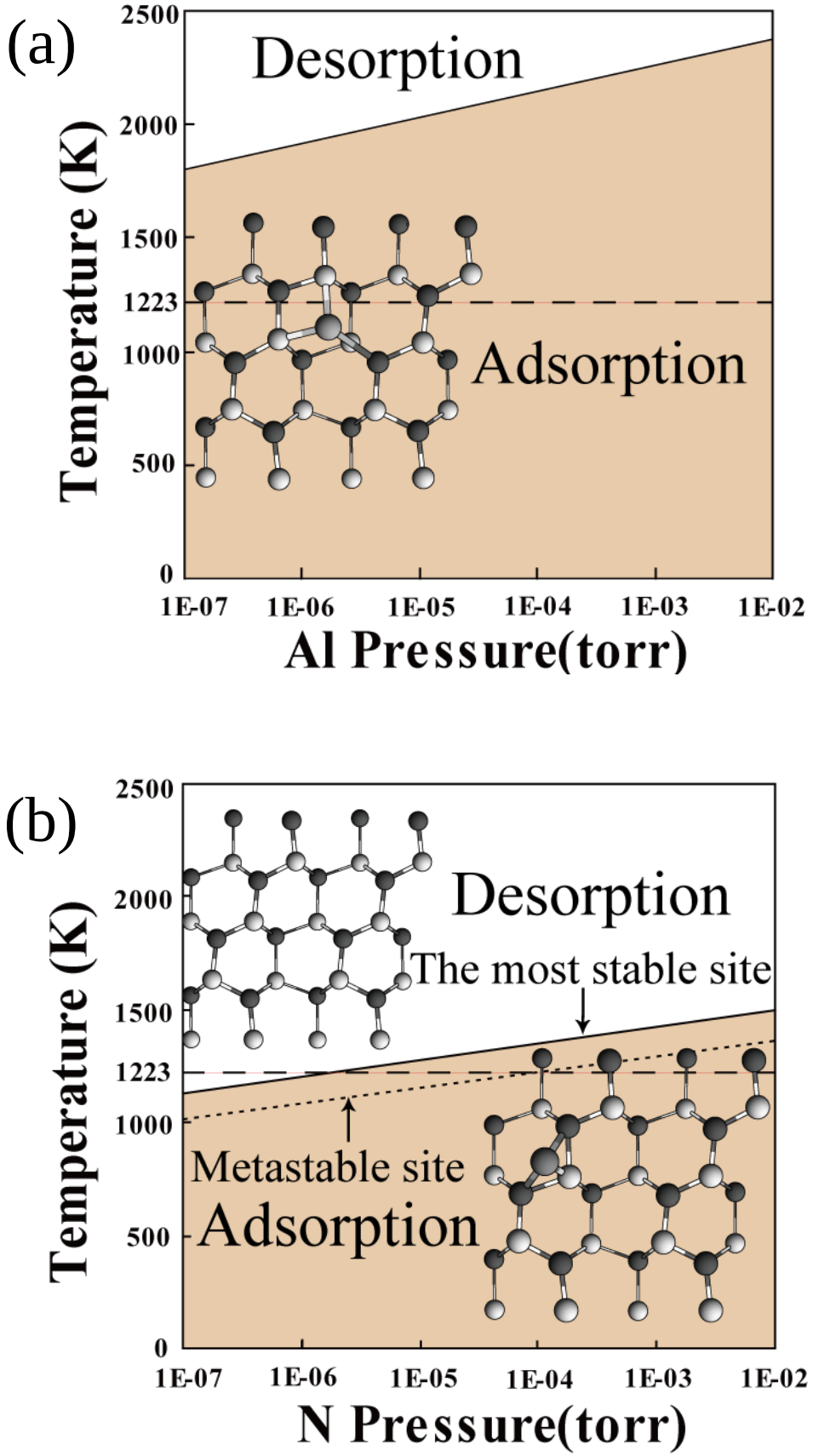
(a)
Desorption
Adsorption
Temperature (K)
2500
2000
1500
1223
1000
500
0
1E-07
1E-06
1E-05
1E-04
1E-03
1E-02
Al Pressure(torr)
(b)
Desorption
The most stable site
Metastable site
Adsorption
Temperature (K)
2500
2000
1500
1223
1000
500
0
1E-07
1E-06
1E-05
1E-04
1E-03
1E-02
N Pressure(torr)